

# Structure and non-collinear magnetism of iron linear chains

N. Fujima<sup>1,a</sup> and T. Oda<sup>2</sup>

<sup>1</sup> Faculty of Engineering, Shizuoka University, Hamamatsu 432-8561, Japan

<sup>2</sup> Faculty of Science, Kanazawa University, Kanazawa 920-1192, Japan

Received 10 September 2002

Published online 3 July 2003 – © EDP Sciences, Società Italiana di Fisica, Springer-Verlag 2003

**Abstract.** Atomic structures and non-collinear magnetic moments are calculated by the first principle molecular dynamics for Fe<sub>5</sub> and Fe<sub>6</sub> linear chains with several fixed and free chain-lengths. The dimerization appears in the optimized atomic structures of all the chains. For the Fe<sub>5</sub>, the magnetic arrangement is parallel for a large chain-length and changes to non-collinear with decreasing the chain-length. For the Fe<sub>6</sub>, the magnetic arrangement is antiparallel in a unit of dimer for a small chain-length and changes to non-collinear with increasing the chain-length. These magnetic behaviors are simulated by a simple  $J_1$ - $J_2$  Heisenberg model.

**PACS.** 31.15.Ar Ab initio calculations – 36.40.Cg Electronic and magnetic properties of clusters – 73.22.-f Electronic structure of nanoscale materials: clusters, nanoparticles, nanotubes, and nanocrystals – 75.75.+a Magnetic properties of nanostructures

## 1 Introduction

Many types of atomic scale materials have been produced in the recent progress of nano-technology. These materials such as the nano-wires [1] have been expected not only to be industrially applied, but also to have new quantized features [2,3]. The magnetic property in nano-wire of transition metal is especially interesting because of the low dimensional and anomalous geometrical structures, which lead to giant and frustrated magnetic moments. Morigaki *et al.* have revealed, in their calculation with the Hubbard model, that the magnetic property changes from paramagnetic to ferromagnetic and *vice versa* as the wire is stretched [4]. It also has been revealed, by the non-collinear local spin-density calculation, that the magnetic moment of the Fe<sub>3</sub> linear cluster has a non-collinear magnetic property, where the magnetic moments of the both end atoms tilt almost perpendicularly to that of the center atom [5,6]. This result suggests that effective antiferromagnetic interaction is very large between the end atoms (between the second neighbors). It is expected that long-range non-collinear magnetic arrangements appear also in longer chains.

In the present paper, we calculate the atomic structures and magnetic moments of Fe<sub>5</sub> and Fe<sub>6</sub> linear chains by the non-collinear first principle molecular dynamics, and discuss the non-collinear magnetic properties as the chain-length is changed. It is shown that the optimized structures have a dimerization for both the chains. It is also shown that the magnetic moments of Fe<sub>5</sub> align parallel for the large chain-length and gradually tilt from center

to the ends with decreasing the chain-length, and that the magnetic moments of Fe<sub>6</sub> align antiparallel in a unit of dimer for small chain-length and tilt with increasing the chain-length.

As a preliminary work, we calculated the non-collinear magnetic moments of Fe<sub>5</sub> and Fe<sub>7</sub> linear chains with fixed equal interatomic distances by the discrete variational local spin-density functional method [7]. In that work, we have obtained some non-collinear magnetic arrangements. However, the calculation has not included the effect of dimerization, which may play an important role in the magnetic property. It is mentioned that Chen *et al.* found a tightly bound Cr dimer to play a key role in determining the structures of small Cr clusters [8].

## 2 Calculations

All the calculations in the present work are performed by the first principle molecular dynamics [5,9], in which the generalized spin-density functional method is employed [10]. In this method, the eigenstates are described by two component complex wave functions,  $\Psi_i = \{\psi_{1i}, \psi_{2i}\}$ , which generate the  $2 \times 2$  non-collinear density matrix  $\rho(\mathbf{r})$ . The elements of  $\rho$  are defined as

$$\rho_{\alpha\beta}(\mathbf{r}) = \sum_i f_i \psi_{\alpha i}(\mathbf{r}) \psi_{\beta i}(\mathbf{r}). \quad (1)$$

Here,  $\alpha$  and  $\beta$  are spin indices and  $f_i$  is the occupation number of the  $i$ th eigenstate.  $\rho$  is decomposed by the Pauli

<sup>a</sup> e-mail: tsnfuji@ipc.shizuoka.ac.jp

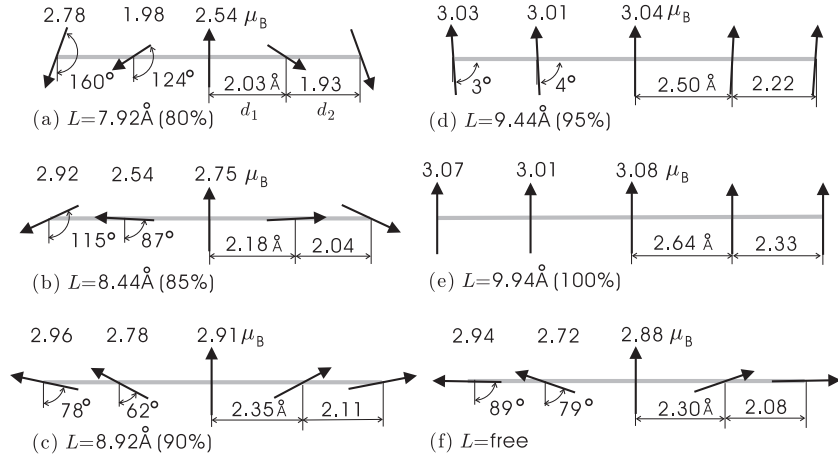


**Fig. 1.** Interatomic distance and magnetic moment of Fe<sub>5</sub> chain.

matrices,  $\sigma_q, (q = x, y, z)$ ;

$$\rho(\mathbf{r}) = \frac{1}{2}n(\mathbf{r})\mathbf{I} + \frac{1}{2}\sum_q m_q(\mathbf{r})\sigma_q, \quad (2)$$

where  $\mathbf{I}$  is the unit matrix,  $n$  and  $\mathbf{m} = (m_x, m_y, m_z)$  are the charge density and spin density vector, respectively.  $\rho(\mathbf{r})$  is oriented to the local spin axis determined from  $\mathbf{m}(\mathbf{r})$ .

The electronic wave functions  $\{\Psi_i\}$  and the atomic positions  $\{\mathbf{R}_I\}$  are simultaneously optimized by solving the equations of motion for  $\Psi_i$  and  $\mathbf{R}_I$  with the ultrasoft pseudopotential scheme [11]. In this scheme, the density matrix has a hard augmented component, so that equation (1) is modified with the augmentation electron density. The wave functions and the density matrix are expanded into a set of plane waves with a cutoff energy of 24 and 250 Ry, respectively. The usual local exchange-correlation potential [12] is applied to the densities,  $n(\mathbf{r})$  and  $m(\mathbf{r})$ . Details of the calculation are described in references [13,14].

We employ two types of chains. First, the chain length,  $L$ , is fixed at  $L = 7.92\text{--}9.94 \text{ \AA}$  for Fe<sub>5</sub> and  $L = 9.94\text{--}12.41 \text{ \AA}$  for Fe<sub>6</sub>, as shown in Figures 1a–1e and 2a–2e. These lengths correspond to those with 80–100% interatomic distance of the Fe bulk crystal (2.48 Å). Second, the boundary atoms are freely moved from the initial length of  $L = 8.92 \text{ \AA}$  for Fe<sub>5</sub> and  $L = 11.16 \text{ \AA}$  for Fe<sub>6</sub>. The atomic positions are initiated from an equal interatomic distance for each chain. These chains are set on a diagonal of a simple cubic unit cell with a lattice constant of 20 a.u. No symmetrical restriction is applied in the calculation. However, the geometrical structure keeps linear during the optimization since the forces between the atoms occur only along the linear chain.

## 3 Results

### 3.1 Fe<sub>5</sub> chain

Figure 1 shows the optimized interatomic distances and the magnetic moments of the Fe<sub>5</sub> chain: Figures 1a–1e for

the fixed chain-lengths,  $L = 7.92\text{--}9.94 \text{ \AA}$ , and Figure 1f for the optimized chain-length. In the figure, the interatomic distances (Å) are indicated on the right-hand side of each chain, the absolute magnetic moments ( $\mu_B$ ) and their angles (degree) relative to that of the center atom are indicated on the left-hand side.

The calculation shows that the optimized interatomic distance between the end and the next atoms,  $d_2$ , is shorter than that between the central and the neighbor atoms,  $d_1$ , for all the chains. That is, a dimerization, which corresponds to the Peierls distortion, occurs at both the ends. The dimer length,  $d_2$ , changes from 1.93 to 2.33 Å with increasing the chain-length, and the ratio,  $d_2/d_1$ , changes from 0.95 to 0.88.

The magnetic moment at each atom aligns parallel each other for  $L = 9.94 \text{ \AA}$  in Figure 1e, and the direction of magnetic moment on each side rotates oppositely with decreasing the chain-length. The arrangement of the magnetic moment becomes non-collinear (but coplanar); the angle at the end atom (at the next) becomes 124° (160°) for  $L = 7.92 \text{ \AA}$  in Figure 1a. It is expected that the magnetic arrangement will become antiparallel when the chain-length becomes shorter. This change in magnetic arrangement can be understood by the competition between the ferromagnetic and antiferromagnetic interactions: ferromagnetic interaction between the first neighbors, and the antiferromagnetic interaction between the second neighbors. This competition will be discussed by a  $J_1\text{--}J_2$  Heisenberg model in the following section.

The optimized chain-length is 8.76 Å ( $d_1 = 2.30$ ,  $d_2 = 2.08$ ) as shown in Figure 1f. The magnetic moments of both the end atoms are almost antiparallel each other and perpendicular to that of the central atom. This arrangement is similar to that of the Fe<sub>3</sub> linear chain, where the angle of the magnetic moments between the central and the end atoms is 84° [5].

### 3.2 Fe<sub>6</sub> chain

Figure 2 shows the interatomic distances and the magnetic moments of the Fe<sub>6</sub> chain: Figures 2a–2e for the

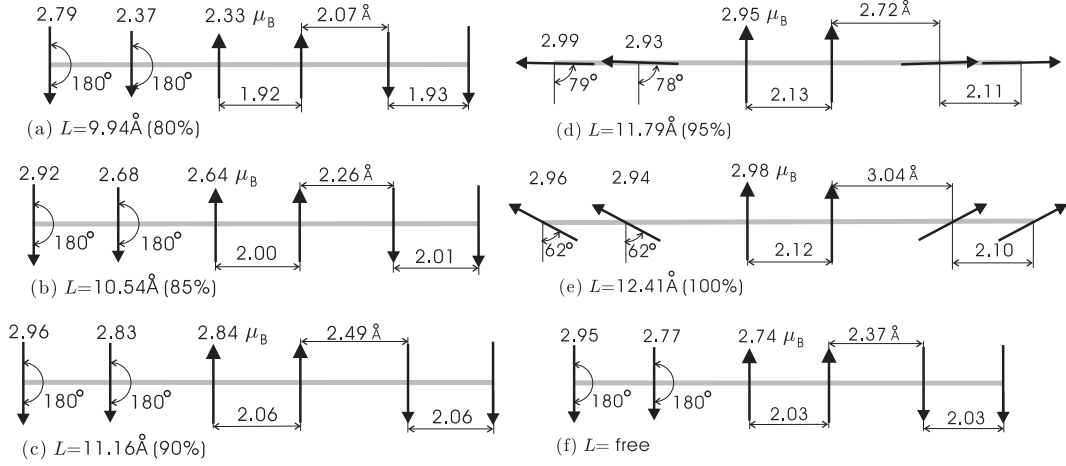


**Fig. 2.** Interatomic distance and magnetic moment of  $\text{Fe}_6$  chain.

fixed chain-lengths,  $L = 9.92\text{--}11.94$  Å, and Figure 2f for the optimized chain-length.

The optimized structure is composed of three dimers whose interatomic distances are almost the same. The interatomic distance of the dimer change from 1.93 to 2.13 Å with increasing the chain-length, while the distance between the dimers changes from 2.07 to 3.04 Å. The ratio of these distances changes from 0.93 to 0.69. Therefore, the dimerization is stronger in the  $\text{Fe}_6$  than in the  $\text{Fe}_5$  (0.95 ~ 0.88). This is due to the fact that the existence of a monomer weakens the dimerization in the  $\text{Fe}_5$ .

The magnetic moments within each dimer align parallel for all the chain-lengths, and so the magnetic moment behaves in a unit of dimer. The magnetic moments of the dimers align antiparallel for  $L \leq 11.16$  (including the optimized chain-length, 10.83 Å) as shown in Figures 2a–2c and 2f. The magnetic moments of the dimer on each side rotate oppositely (but coplanarly) with increasing the chain-length; the angle between the central and side dimers is about  $80^\circ$  for  $L = 11.79$  Å in Figure 2d, and  $60^\circ$  for  $L = 12.41$  Å in Figure 2e. They will align parallel when the interdimer distance is widened more.

The size-dependence of magnetic arrangement of the  $\text{Fe}_6$  in Figure 2 seems to be different from that of the  $\text{Fe}_5$  in Figure 1. However, both the magnetic arrangement can be explained qualitatively by a  $J_1$ - $J_2$  Heisenberg model with the dimerization as described in the next section.

#### 4 $J_1$ - $J_2$ Heisenberg model

In this section, the magnetic arrangement of the  $\text{Fe}_5$  and  $\text{Fe}_6$  chains are discussed by a  $J_1$ - $J_2$  Heisenberg model. Figure 3 shows schematic diagrams of the model, Figure 3a for  $\text{Fe}_5$  and Figure 3b for  $\text{Fe}_6$ . Here,  $J_1$  indicates an effective ferromagnetic interaction within a dimer,  $J'_1$  a ferromagnetic interaction outside a dimer,  $J_2$  and  $J'_2$  antiferromagnetic interactions between the second neighbors. Assuming the coplanar arrangement, the interaction Hamiltonians,  $H'_5$  for  $\text{Fe}_5$  and  $H'_6$  for  $\text{Fe}_6$ , are expressed

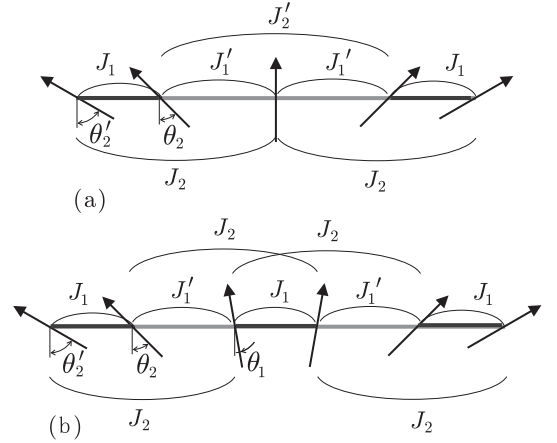


**Fig. 3.**  $J_1$ - $J_2$  Heisenberg dimer model: (a) for  $\text{Fe}_5$  and (b) for  $\text{Fe}_6$ .

as follows:

$$H'_5 = -2J_1 \cos(\theta_2 - \theta'_2) - 2J'_1 \cos \theta_2 + 2J_2 \cos \theta'_2 + J'_2 \cos 2\theta_2 \quad (3)$$

$$H'_6 = -J_1 \{ \cos 2\theta_1 + 2 \cos(\theta_2 - \theta'_2) \} - 2J'_1 \cos(\theta_1 - \theta_2) + 2J_2 \{ \cos(\theta_1 + \theta_2) + \cos(\theta_1 - \theta'_2) \}, \quad (4)$$

where  $\theta_1$  is the angle of the magnetic moment of the two atoms around the center of the  $\text{Fe}_6$ ,  $\theta'_2$  and  $\theta_2$  are those of the end and the next atoms, respectively. The magnetic arrangement can be decided by minimizing equations (3) or (4) with a certain set of parameters,  $J_s$ .

Figure 4 shows  $\theta_2$ (degree) at the minimum of  $H'$  as the function of  $J'_1/J_1$  and  $J_2/J_1$ : Figure 4a for  $\text{Fe}_5$  with  $J'_2/J_2 = J'_1/J_1$  and Figure 4b for  $\text{Fe}_6$ . The horizontal axis,  $J'_1/J_1$ , means the degree of dimerization; no dimerization occurs when  $J'_1/J_1 = 1$ , and dimers are completely separated when  $J'_1/J_1 = 0$ . The vertical axis,  $J_2/J_1$ , indicates the degree of the antiferromagnetic interaction between the second neighbors.

In the black area at the bottom, where  $\theta_2 = 0$ , all the magnetic moments are parallel as shown in Figure 1e

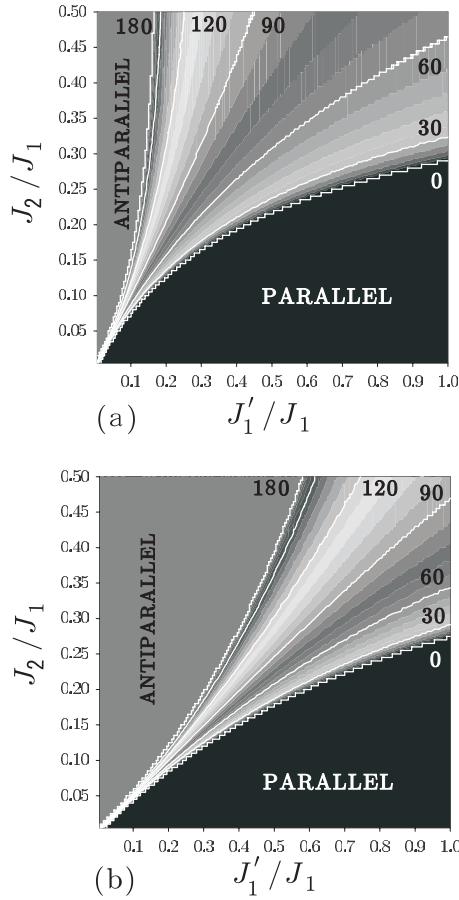


**Fig. 4.** Angle of the magnetic moment  $\theta_2$  at the minimum of  $H'$ : (a) for  $\text{Fe}_5$  and (b) for  $\text{Fe}_6$ .

although the other angles,  $\theta_1$  and  $\theta'_2$ , are not shown. In the gray area at the left-hand side, where  $\theta_2 = 180$ , the magnetic moment of each dimer aligns antiparallel as shown in Figure 2a. The magnetic arrangement is non-collinear in the other area where  $0 < \theta_2 < 180$ . It is noted that no antiferromagnetic alignment occurs in the region where  $J'_1/J_1 \approx 1$  (in the region where the dimerization is weak). This agrees with the preliminary results for the chain with an equal interatomic distance [7].

For the  $\text{Fe}_5$  chain in Figure 4a, the area of the antiparallel alignment is small and the area of the parallel alignment is predominant. (This tendency is more obvious when  $J_2 = J_1$ .) By contrast, the antiparallel area is significant for the  $\text{Fe}_6$  chain in Figure 4b. Moreover, the non-collinear area is smaller in Figure 4b than in Figure 4a. Because no interaction exists between the second nearest dimers across a dimer in the present  $J_1$ - $J_2$  model, it is easy for the  $\text{Fe}_6$  to realize the antiparallel alignment of dimer (the parallel alignment between the second nearest

dimers) as in Figure 2f. On the other hand, the antiferromagnetic interaction,  $J_2$ , exists between two dimers across a monomer, so it is difficult for the dimers in the  $\text{Fe}_5$  to align parallel, but easy to tilt each other as in Figure 1f. The simulation by the  $J_1$ - $J_2$  model qualitatively agrees with the results obtained by the first principle molecular dynamics, where no antiparallel alignment appears for the  $\text{Fe}_5$  in Figure 1 and that is predominant for the  $\text{Fe}_6$  in Figure 2 although the actual parameters,  $J_s$ , are not clearly determined by the model.

## 5 Conclusion

Atomic structures and non-collinear magnetic moments are calculated by means of the first principle molecular dynamics for the  $\text{Fe}_5$  and  $\text{Fe}_6$  linear chains. The calculation shows that the optimized atomic structures have the dimerization and the magnetic arrangement also has a unit of dimer, especially for the  $\text{Fe}_6$ . However, the existence of a monomer weakens the dimerization and brings the gradually tilt magnetic arrangement for the  $\text{Fe}_5$ . It is expected that the existence of a monomer has a great effect on the magnetic arrangement not only for the  $\text{Fe}_5$  but also for longer chains. That is, the magnetic arrangement of the Fe chain depends on whether the number of atoms is even or odd.

## References

1. H. Ohnishi, Y. Kondo, K. Takayanagi, *Nature* **395**, 780 (1998)
2. L. Olesen, E. Lægsgaard, I. Stensgaard, F. Besenbacher, J. Schiøtz, P. Stoltze, K.W. Jacobsen, J.K. Nørskov, *Phys. Rev. Lett.* **72**, 2251 (1994)
3. J.L. Costa-Krämer, *Phys. Rev. B* **55**, R4875 (1997)
4. Y. Morigaki, H. Nakanishi, H. Kasai, A. Okiji, *J. Appl. Phys.* **88**, 2682 (2000)
5. T. Oda, A. Pasquarello, R. Car, *Phys. Rev. Lett.* **80**, 3622 (1998)
6. D. Hobbs, G. Kresse, J. Hafner, *Phys. Rev. B* **62**, 11556 (2000)
7. N. Fujima, T. Oda, *Trans. MRS-J* **27**, 201 (2002)
8. H. Chen, L.-S. Wang, *Phys. Rev. Lett.* **77**, 51 (1996)
9. R. Car, M. Parrinello, *Phys. Rev. Lett.* **55**, 2471 (1985)
10. J. Kübler, K.-H. Höck, J. Sticht, A.R. Williams, *J. Phys. F* **18**, 469 (1988)
11. D. Vanderbilt, *Phys. Rev. B* **41**, 7892 (1990)
12. J.P. Perdew, A. Zunger, *Phys. Rev. B* **23**, 5048 (1981)
13. K. Laasonen, A. Pasquarello, R. Car, C. Lee, D. Vanderbilt, *Phys. Rev. B* **47**, 10142 (1993)
14. T. Oda, *J. Phys. Soc. Jpn* **71**, 519 (2002)